



# The determination of skin surface pH via the skin volatile emission using wearable colorimetric sensors

Finnegan M., E. Duffy, A. Morrin\*

School of Chemical Sciences, Insight SFI Research Centre for Data Analytics, National Centre for Sensor Research, Dublin City University, Ireland

## ARTICLE INFO

### Keywords:

Wearable  
Colorimetric sensor  
Skin surface pH  
Volatile fatty acids  
Ammonia  
Gland secretions  
Euclidean distance

## ABSTRACT

Biodiagnostic sensors in the form of wearables have become of widespread interest in both the scientific and clinical communities in recent years due to their potential for monitoring human health, well-being and physical performance. However, collecting biofluids from the skin to enable biochemical analysis using wearables has proved challenging to date. This research seeks to overcome the need for fluid collection by designing a wearable sensing platform capable of monitoring the volatile emission from skin with the aim of collecting biodiagnostic information from the body. We investigate the use of a simple wearable colorimetric sensing platform incorporating sensor spots comprising encapsulated bromocresol green pH indicator dye in an enclosed headspace above the skin. The sensor spots undergo a colour change in response to basic volatile nitrogen compounds such as ammonia and amines being emitted from skin. By deploying this wearable in a healthy participant study, a strong correlation between sensor colour response and skin surface pH was demonstrated, despite a significant inter-individual variability being noted. Sensor response was observed to be highly dependent on gender as well as body site, and attributed to factors such as gland and microbial composition differences. Finally, the wearable's ability to detect changes in skin surface pH in response to topical skin treatments was demonstrated. Overall, this work demonstrates a novel and simple approach to wearable biodiagnostics that exploits the skin volatile emission to monitor skin physiology without the need for microneedles or the requirement to harvest fluid from the skin.

## 1. Introduction

The skin is the largest organ of the human body with a high surface area of 1.5–2 m<sup>2</sup> [1], making it readily accessible as an organ to perform diagnostics on and as such, has been exploited as a matrix for a range of wearable sensing approaches to date [2]. The stratum corneum (SC) is the outer layer of the epidermis of the skin hosting a rich set of biomarkers and a high metabolic activity [3]. Quantifying levels of various biomarkers present in skin fluid matrices [4] such as interstitial fluid (ISF) [5] and sweat [6] can provide valuable insights into the health of an individual. Indeed, these opportunistic fluid matrices within skin have given rise to the fabrication and development of epidermal platforms [7] engineered to extract these biofluids from skin for detection of biomarkers including the hydrogen ion [8], glucose [9,10], lactate [11,12], sodium [12,13], potassium [13], ammonia [14] and urea [15].

ISF, for example, is considered as an alternative to blood for accessing systemic biomarkers of disease. Small molecules such as lactate, glucose, cortisol and urea are present in ISF and measuring their

concentrations and flow patterns can provide information on specific diseases [16]. There are many extraction methods used to extract ISF from skin including suction blister, iontophoresis, sonophoresis and microdialysis, none of which are immediately straight-forward [17]. Most recently microneedles (MNs) have been developed to extract and collect ISF from skin. Goud et al. have recently developed a wearable microneedle device for the continuous sensing of levodopa, a drug used to treat Parkinson's disease, in ISF [18]. A microneedle electrode array which penetrates the skin is used and allows for dual-mode sensing involving both redox and biocatalytic processes. However, this approach is far from being clinically available as trials were only carried out on mice, and human participant testing remains to be done. In addition to this, MNs have the drawback of damaging the skin by puncturing and thus can potentially induce immunological responses giving rise to localised skin irritation and even infection.

Sweat is a more accessible skin matrix that can be sampled non-invasively. In a similar manner to ISF, it can provide information about human health by analysis of the biomarkers it contains. The

\* Corresponding author.

E-mail address: [aoife.morrin@dcu.ie](mailto:aoife.morrin@dcu.ie) (A. Morrin).

<https://doi.org/10.1016/j.sbsr.2022.100473>

Received 18 September 2021; Received in revised form 22 December 2021; Accepted 4 January 2022

Available online 6 January 2022

2214-1804/© 2022 The Authors. Published by Elsevier B.V. This is an open access article under the CC BY license (<http://creativecommons.org/licenses/by/4.0/>).

SWEATCH wearable platform is an exciting example of this and was developed to harvest and analyse sodium concentration in sweat in real-time [19]. This electrochemical approach is comprised of a pod-like design which incorporates an ion-selective electrode for sodium detection. It also integrates a fluidic system, driven by capillary forces, to collect sweat from the skin, directing its flow over the electrodes for detection. Recently, the SWEATCH platform has been further developed, facilitating the detection of sodium and potassium ions simultaneously [20]. The detection of the hydrogen ion in sweat has also been targeted with wearable sensing devices. A recent demonstration of a single-use colorimetric wearable sensor integrating detection of several analytes including sweat pH was recently reported by the group of Rogers using a skin-interfaced microfluidic/electronic system [21]. This colorimetric approach uses pH-responsive universal indicator dye dip-coated on filter paper to determine sweat fluid pH. As with the SWEATCH, participants were asked to exercise to induce sweating. Produced sweat is then manipulated through hollow microfluidic channels, again by capillary force action, and routed to the pH sensor for detection. A smartphone is used to image the colour sensor after sampling, and images compared to reference markers to determine sweat pH. Approaches to sweat diagnostics such as these, rely on microfluidic architecture to guide the sweat to the sensing interface for analysis which can lead to complexities. Furthermore as these approaches, along with many others [22] requires the generation of sweat, they are thus suited more to sports applications than routine health diagnostics.

The analysis of volatile compounds emanating from the skin is emerging as an interesting source of information regarding subcutaneous and even systemic biochemistry [3]. These volatiles are derived from glandular secretions and their interactions with the microflora of the skin. Over 600 compounds have been reported to be emitted as volatiles from skin [23,24]. Skin volatiles are sampled non-invasively [25,26] without the need to puncture skin as often required for ISF collection for example. Compared to sweat, volatile emissions are a more accessible skin matrix as the volatiles are passively emitted and can be collected easily [27,28]. Our group has been studying the skin volatile emission for several years [3,29,30] using gas chromatography–mass spectrometry (GC–MS) workflows and we have recently established evidence of a correlation between the emission rate of volatile fatty acids (VFAs) from skin and skin surface pH [31]. Skin surface pH is a parameter of interest as changes in this parameter can indicate dysregulation of the skin barrier function and alterations in skin surface pH can play a role in the pathogenesis of skin conditions such as atopic dermatitis [32,33]. Healthy human skin has an acidic surface pH of between 4.0 and 6.0 [1]. The acidic nature of the SC is important both for permeability barrier function and cutaneous antimicrobial defence. The acidic pH of the skin surface is established by several key mechanisms [34]: the breakdown of the filaggrin gene to produce transurocanic acid, the sodium proton exchanger - a transporter protein which transports  $H^+$  ions to the SC and the hydrolyzation of free fatty acids (FFAs) from phospholipids by phospholipases.

Ammonia in the human body stems primarily from the bacterial breakdown of proteins within cells and the intestine. It is transported by blood to the liver where it is converted to urea and ultimately washed out in urine. Ammonia remaining in the blood can diffuse through the SC [35] or be emitted in eccrine sweat [15]. Total ammonia consists of two principal forms, the ammonium ion ( $NH_4^+$ ) and un-ionised free ammonia ( $NH_3$ ), with relative concentrations being pH- (and temperature-) dependent. Within the SC, ammonia production is probably not high enough to affect large pH changes in the skin. However,  $NH_4^+$  is present in eccrine sweat gland secretions [15] and converts to gaseous  $NH_3$  in a pH-dependent manner. Ammonia may also be produced microbially on the skin surface, for example from the action of microbial urease enzyme on urea substrate (present in sweat [36,37]). Volatile amines such as triethylamine and ethanolamine are also emitted from skin, and are likely again microbially-derived [38]. Longer chain amines in the skin volatile emission have also been reported but their origin is

not certain [29,39]. Overall, it is ammonia that is thought to contribute most significantly as a basic volatile nitrogen compound to the skin emission and this has been studied by several groups [35,40,41]. However, interestingly, none of the studies published to date have considered the implication of skin surface pH on ammonia emission flux to our knowledge.

Colorimetric dyes as wearable sensors such as those measuring skin pH have up to now been typically limited to sweat analysis [42–45] and so require sweat-promoting stimulation as well as intricate microfluidics to guide sweat to the localised sensing chemistries for detection. This work proposes measuring of the skin surface pH via the volatile ammonia emission in a simple colorimetric sensor format. It is based on the principle that the  $NH_4^+/NH_3$  equilibrium in skin is pH dependent. Thus, it could be expected that by monitoring the flux of gaseous ammonia from skin, it would provide a measure of skin surface pH. To this end, a simple sensor platform, comprising spots of encapsulated pH-responsive dye, bromocresol green (BCG) (in acid form), was worn above the skin within an enclosed headspace (HS) and the colour response to the skin volatile emission monitored. The colour changes observed were consistent with dye deprotonation and are attributed principally to the pH-dependent skin volatile ammonia emission. Given the observed correlation of sensor response to the underlying skin surface pH, this offers an interesting sensing approach that has advantages over other methods measuring skin pH that require sweat fluid extraction and collection. It opens up the possibility of this volatile compound emission sensing approach as a way to detect other biomarkers that may have diagnostic value. This work deepens our understanding of the initial concept reported earlier [31], and investigates the wearable sensor's ability to accurately measure skin surface pH and the various factors that influence the measurement including gender, body site, measurement time and topical treatment of skin. The outcome of this work provides an understanding of some of the key factors and challenges impacting the sensor's response behaviour when worn on the body, while also highlighting the potential of monitoring other components of the volatile emission using selective encapsulated colour chemistries as a non-invasive and facile approach to skin diagnostics.

## 2. Materials and methods

### 2.1. Preparation of colorimetric sol-gel

Colorimetric sol-gel solution was prepared according to a previously published protocol [46]. Briefly, sol-gel was prepared by mixing 126  $\mu$ L triethoxy(octyl)silane, 40  $\mu$ L methyltriethoxysilane, 304  $\mu$ L hydrochloric acid (0.1 M), 384  $\mu$ L 2-methoxyethanol and 272  $\mu$ L propylene glycol monomethyl ether acetate in a reaction vessel and stirring overnight. 4 mg bromocresol green (BCG) was then dissolved in the sol-gel (1000  $\mu$ L).

### 2.2. Solution-based pH study

20  $\mu$ L of the BCG sol-gel solution was added to vials containing bulk solutions (2800  $\mu$ L) of varying pHs (3.2–7.0) prepared using 0.01 M HCl and 0.01 M NaOH stock solutions. A calibrated HI-1131B pH electrode (Hanna Instruments) was used to determine the pH of each vial solution. A reference solution (pH 2.50), containing 20  $\mu$ L BCG sol-gel diluted in 2800  $\mu$ L 2-methoxyethanol, was also prepared. Imaging of the vials was done using an iPhone 11 Pro Max and images processed as described below.

### 2.3. Preparation of colorimetric sensor spots

0.5  $\mu$ L of the BCG sol-gel solution was drop-cast as a single spot onto a 10% acetate cellulose thin layer chromatography (TLC) plate (Macherey-Nagel, Fischer Scientific, Ireland) (3 × 2 cm) and allowed to dry in a vacuum desiccator before use. 6 spots, approx. 1 cm apart, were drop-cast onto each cellulose substrate to form a 3 × 2 colorimetric

sensor array of replicate spots.

#### 2.4. Colorimetric sensor response to ammonia

The colorimetric sensor was prepared (comprising 6 replicate BCG spots drop-cast on substrate as described above), scanned and the RGB values of the individual spots quantified using ImageJ. In order to measure the response of the sensor spots to ammonia, the sensor was adhered to the lid of a plastic petri dish (0.04 L) using Blu-Tack. A piece of filter paper (Whatman, diameter: 4.70 cm) was placed in the bottom of the petri dish and a precise volume of neat ammonia solution (0.1–10  $\mu\text{L}$ ) was dropped directly onto the filter paper. The lid was placed on top of the petri dish and sealed with parafilm. After 3 h, the sensor was removed from the petri dish and scanned. Processing of the sensor image before and after exposure to ammonia was carried out using ImageJ as described below.

#### 2.5. Preparation of the wearable platform

The wearable platform comprised a stainless steel woven wire mesh (Inoxia Ltd., UK) to define the headspace ( $4 \times 3$  cm), on top of which was the cellulose substrate comprising of 6 replicate BCG sensor spots. The sensor spots were covered with a polyethylene terephthalate (PET) film ( $5 \times 4$  cm) and the complete platform was enclosed (Fig. 1(a)) and secured to a body site using Leukosilk surgical tape (BSN Medical GmbH, Hamburg, Germany).

#### 2.6. Wearable colorimetric sensor participant study

Ten healthy volunteers (5 female and 5 male; aged 20–45) were recruited onto this study (see Consort Diagram, Scheme 1). Participants were instructed not to apply perfumes or cosmetics to their body on the days of sample collection. Participants were informed on the aim and purpose of the study, and asked to provide written informed consent. The local ethics committee (Dublin City University Research Ethics Committee) approved the study on skin volatiles (Reference: DCUREC/2016/053) prior to commencement of the work, and the study was

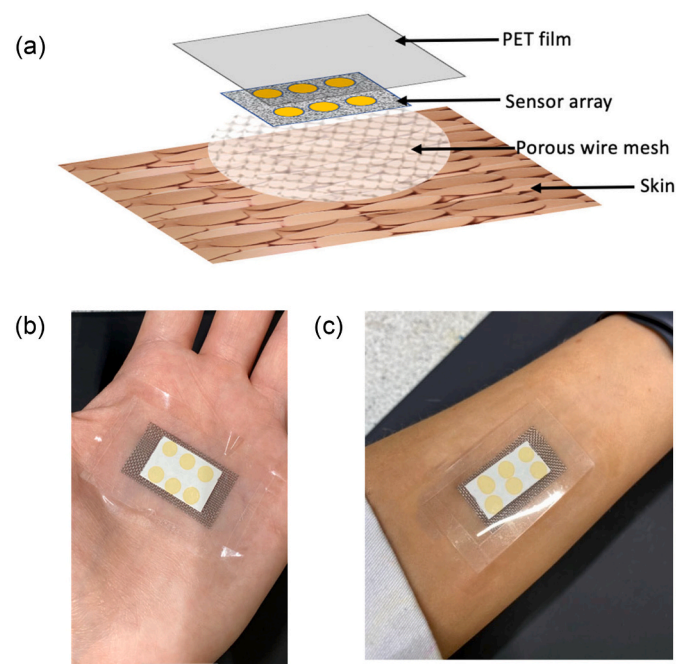


Fig. 1. (a) Schematic of the different layers comprising the wearable platform applied to the skin surface [31]; (b) image of wearable platform worn on palm and (c) on the forearm.

performed according to the Declaration of Helsinki.

Prior to application of the wearable platform to participant's skin, an image of the replicate BCG sensor spots was taken using an Epson XP-322 flatbed scanner. Participants were then asked to apply the wearable platform to a specific skin site (palm of hand, sole of foot, forehead or stomach) for up to 300 min while they went about their daily activities. After a fixed time, the wearable was removed from the skin and the sensor spots imaged again using the scanner. Where specified, the wearable was removed from the skin periodically (i.e., every 15 min) and the sensor spots imaged using the scanner before being replaced on the skin.

Skin surface pH of each site was taken before application of the wearable platform using a wireless HALO flat glass probe (HI14142) (Hanna Instruments) and Hanna Lab App (v3.0) for iPhone.

#### 2.7. Skin treatment study

Four different skin treatments were carried out on the palm to investigate their impact on sensor colour response. The treatments were (a) washing the skin with soap (Dove Beauty Cream Bar), (b) applying a 2% salicylic acid (SA) solution (The Ordinary©), (b) wiping the skin with an isopropyl alcohol (IPA) (Qualicare Products) wipe and (d) tape-stripping of the SC using Leukosilk surgical tape (1.25 cm wide) where the skin was tape stripped 10 times as a single treatment. Following each treatment, the wearable sensor was applied for 120 min and imaged in the usual manner before and after wearing. Skin surface pH was also taken at the site before the wearable was applied.

#### 2.8. Image analysis

Images were analysed using ImageJ to measure absolute red (R), green (G) and blue (B) colour values for the sensor spots before ( $R_1, G_1, B_1$ ) and after exposure ( $R_2, G_2, B_2$ ) to skin. Sensor spot response was also quantified using a distance measurement called Euclidean distance (ED). The ED formula is given by:

$$ED = \sqrt{(R_2 - R_1)^2 + (G_2 - G_1)^2 + (B_2 - B_1)^2} \quad (1)$$

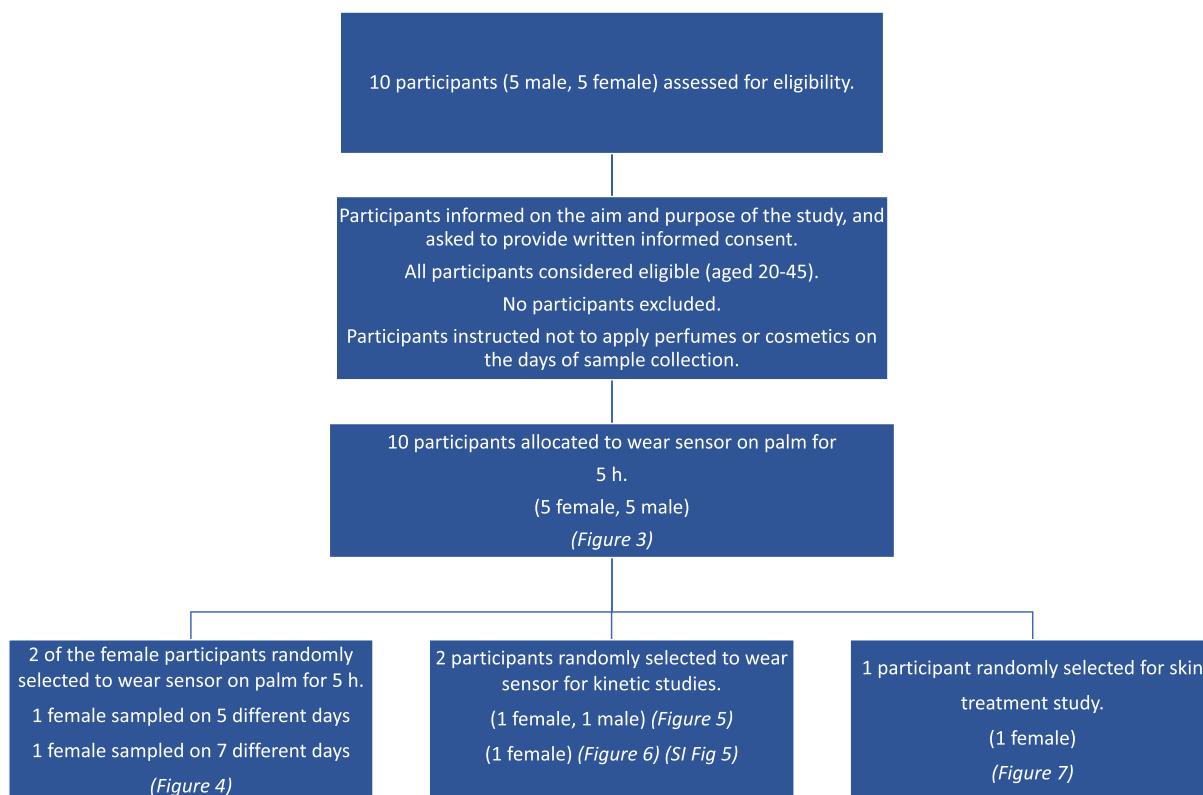
#### 2.9. Data analysis

1-D linear regression analysis was used to investigate the association between sensor spot ED response and skin surface pH. The correlation coefficient, R, was used to quantify association between sensor response and skin surface pH as it is suited to participant studies where variables including age, ethnicity, etc. are not controlled [47].

### 3. Results & discussion

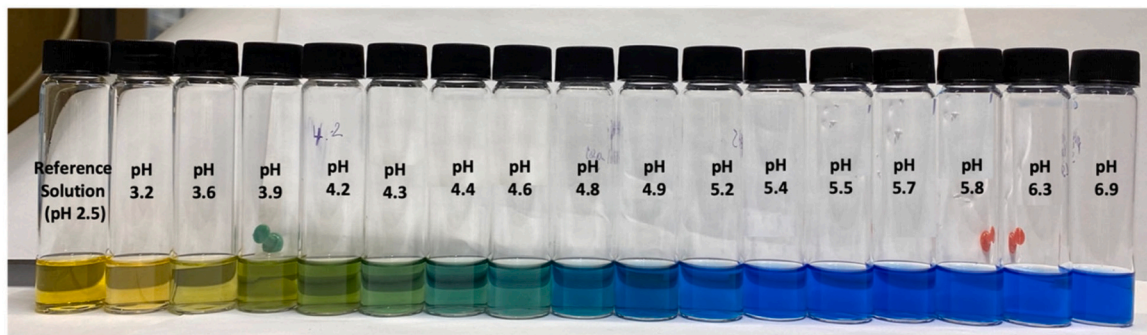
This work investigated the response behaviour of sensor spots comprising an encapsulated pH responsive dye as sensor spots worn above the skin surface targeting the skin volatile emission, with the goal of using it to measure skin surface pH. As the typical pH range for the skin surface is known to be between 4.0 and 6.0, BCG ( $\text{pK}_a = 4.7$ ) was selected as a potentially suitable dye to use for this application. A study of the colorimetric response of prepared BCG sol-gel solutions was carried out in order to verify the dyes response to changes in pH over the relevant range (Fig. 2(a)). ED values obtained from the image processing step were plotted against solution pH to show dye sensitivity between pH 4 and 6 (SI Fig. 1).

To investigate the responsiveness of the BCG as encapsulated sensor spots to ammonia, the sensors were exposed to different masses of ammonia in a HS according to the Methods Section (SI Fig. 2). A quantitative ammonia calibration plot was generated based on sensor ED response whereby correlation with ED response was observed up to a mass of approx. 2.5 mg ammonia (Fig. 2(b)). Beyond this, the sensor



Scheme 1. Consort diagram showing the flowchart for the different aspects of the participant study.

(a)



(b)

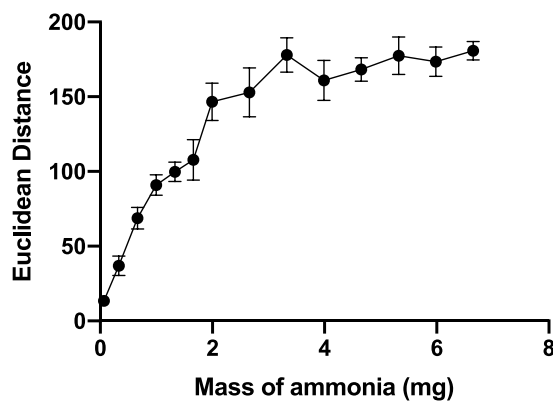


Fig. 2. (a) Image of BCG sol-gel solutions across the pH range 2.5–6.9, and (b) graph showing average ED response as a function of mass of ammonia (mg) added to the HS that the sensor was exposed to. Error bars represent standard deviation in ED response from  $n = 6$  sensor spots on a single substrate.

spots became saturated and no further increase in ED observed. In order to quantify the limit of detection (LOD) of the sensor spots, a narrower mass range of ammonia was used (0.0665–0.6650 mg; (SI Fig. 3)) and linear regression applied to the data to give a linear regression line of  $y = 74.1x + 12.71$ ;  $R = 0.960$ . Based on this regression, the LOD for the sensor was calculated to be 0.092 mg ammonia.

In order to assess how the encapsulated sensor spots responded to the skin emission, the BCG sensor spot substrate was integrated within a wearable platform (Fig. 1), and applied to the palm of healthy participants skin for 5 h and the colour response monitored. Fig. 3(a) shows the average colour of the BCG sensor spots (based on 6 replicate spots from one wearable measurement) after wearing on skin by 5 different female and 5 different male participants with different skin surface pHs. For both genders, it can be seen that the ED response increases with increasing skin surface pH and despite likely inter-person variability, good correlation is seen. The correlated sensor response with respect to pH can be explained by the dependency of ammonia emission flux from the skin on skin surface pH.

Using the standard calibration plot (SI Fig. 3) for ammonia, the ammonia flux ( $\text{mg h}^{-1} \text{cm}^{-2}$ ) for each participant was estimated and the computed values corresponding to the measured pHs are given in Fig. 3 (a). The emission fluxes calculated in this study are higher than previously reported skin ammonia fluxes [35,40,41]. For example, our work reports an average ammonia emission flux for female palm of  $0.0198 \text{ mg h}^{-1} \text{cm}^{-2}$  ( $\pm 0.0113$ ) (based on the average values measured in Fig. 3) whereas Furukawa et al. report an average ammonia flux of  $0.0006 \text{ mg h}^{-1} \text{cm}^{-2}$  for the same site collected using a passive flux sampler with ion chromatographic analysis. A significant disparity arises here but our greater flux estimations may be due to the detection of volatile amines as well as ammonia from skin. In addition, given the occlusion of the skin for our measurements, there is likely some sweat/water vapour being eliminated from the skin containing ammonia and interacting with the sensor spots that could also account for the higher than expected ammonia fluxes measured. No previous study to our knowledge relating to ammonia measurements from skin consider skin surface pH and yet our results show that the ammonia flux can vary by an order of magnitude over the healthy skin surface pH range.

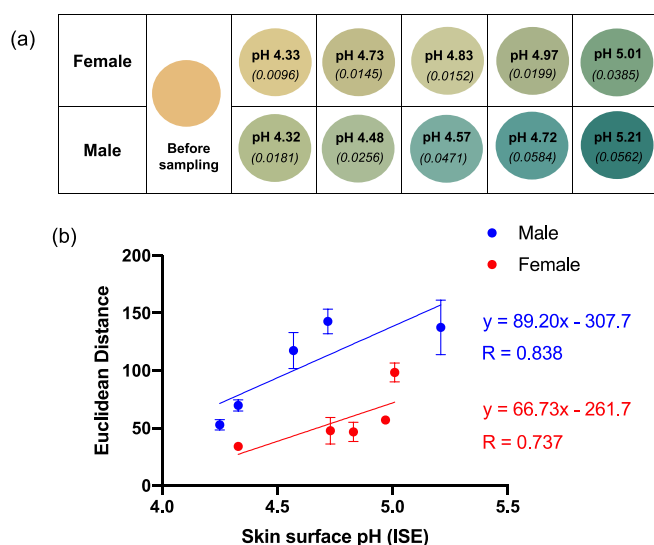


Fig. 3. (a) Reproduced average ED colour response from wearable platform (6 replicate BCG sensor spots) after being worn on 5 females and 5 males (left palm, 5 h); the corresponding skin surface pHs as measured by a calibrated ISE (bold text) and estimated ammonia flux in  $\text{mg h}^{-1} \text{cm}^{-2}$  (italicised text in parenthesis) also given. (b) ED value from (a) plotted as a function of skin surface pH. Error bars represent standard deviation in ED response from  $n = 6$  sensor spots within a single wearable platform. Note: See SI Table 1 for tabulated data.

As noted earlier, a strong gender effect on sensor response can be observed in Fig. 3 where males and females with approximately matched skin surface pH values show different colour responses after exposure to the palm for equivalent times. Males elicited an increased colour response for comparable skin surface pHs compared to females. Although males and females are known to have equivalent numbers of eccrine glands on the palm, the size and volume of sweat produced by these glands is approx. 5 times greater in males compared to females [48]. This increased response in males may be due to higher fluxes of ammonia being emitted from the male eccrine sweat gland on account of the larger gland volumes, as well as potential microbial differences.

In order to investigate the significance of the inter-person variability on sensor response, single participant data was collected on multiple days. For this, 2 participants were randomly selected to wear the sensor as before for fixed periods of time (5 h) on multiple days as outlined in the Consort Diagram (Scheme 1). Fig. 4 demonstrates that ED correlates with pH as expected and that there is significantly increased correlation between ED response and skin surface pH for a single participant compared to Fig. 3 where data from multiple participants was plotted against skin surface pH. This confirms the relationship between sensor ED response and skin surface pH and highlights the inter-person variability as a challenge when designing such sensors.

In order to investigate the kinetic response of the sensor spots, imaging of the sensor was done periodically during the measurement by removing the wearable from the skin every 15 min, imaging the sensor spots, and replacing on the skin immediately after. Corresponding skin surface pH measurements were also taken at these time points, while the wearable was off the skin. Kinetic data at four skin sites - palm, foot, abdomen and forehead - was collected. Skin surface pH data showed that pH did not fluctuate during the measurement period (Fig. 5 a-d) indicating the emission flux of ammonia from the skin remained constant over the period investigated. In general, ED response was observed to increase over time, across all body sites. For all sites, the general trend was that ED continued to increase over time. However, the rate of change of ED differs across the sites, a consistent effect for both males and females. The response differences across the different sites is attributed to differences in skin surface pH but also the microflora and gland type and density present at a particular site. The palm elicited the highest ED response of the sites investigated. The foot resulted in significantly lower responses. However, both the palm and foot are known to have similar eccrine gland densities [49,50] and the measured skin surface pHs for both sites were similar (average measured pH over 300 min: female palm  $4.81 \pm 0.069$ ; female foot  $4.60 \pm 0.063$ ), indicating that the ED response for both sites would be expected to be similar. Thus, it is unclear as to why the ED response is lower for the foot compared to the palm and additional studies would be required to

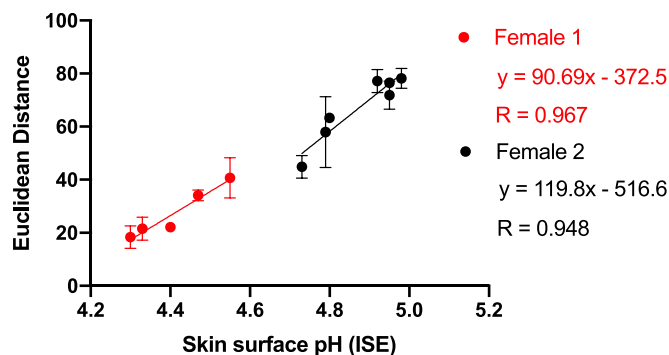
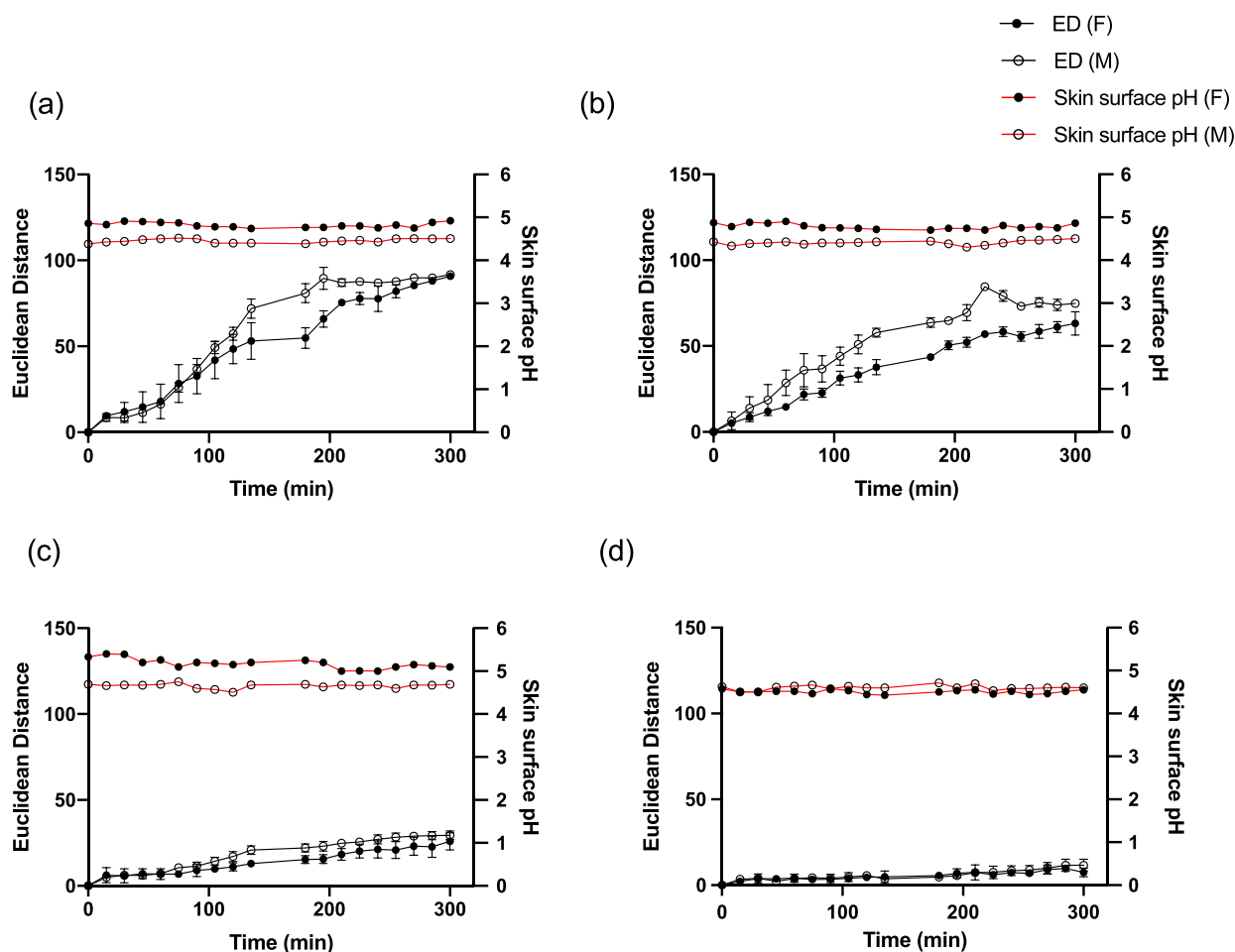


Fig. 4. Average ED response from wearable platform (6 replicate BCG sensor spots) after being worn on Female 1 and Female 2 for 5 h (left palm used for sampling) plotted against skin surface pH (measured using a calibrated ISE). Error bars represent standard deviation in ED response from  $n = 6$  sensor spots within a single wearable platform. Note: See SI Tables 2 and 3 for tabulated data.



**Fig. 5.** Average ED colour response from wearable platform (6 replicate BCG sensor spots) over time on one female and one male participant and corresponding skin surface pH values for (a) palm, (b) foot, (c) abdomen and (d) forehead. Error bars represent standard deviation in ED response from  $n = 6$  sensor spots within a single wearable platform. Note: See SI Tables 4–11 for tabulated data.

further understand this response difference. It may be related to different microbial environments on account of the different exposures to ambient of the site. Interestingly the abdomen had significantly lower ED responses compared to the palm and foot sites despite having a comparable skin surface pH. The stomach has a much lower density of eccrine glands (~2–5 fold lower than that of the palm and foot) [49] likely resulting in a lower net amount of ammonia being produced. The high skin surface pH is most likely driven by the SC acidity regulation mechanisms outlined earlier and ammonia flux is a consequence of this whereby the low density of glands produces less ammonia than other body sites. This is what determines the lower flux of ammonia gas and hence lower than expected sensor response. The microflora on the skin surface may also influence the ED response. The forehead elicited the lowest ED sensor spot responses, indicating the lowest ammonia emission. This site contains the highest density of sebaceous glands and secretions as well as hair follicles (also on the stomach site) [51], which produce significant proportions of FFAs [52] heavily influencing the low skin surface pH (average measured pH over 300 min: female  $4.50 \pm 0.045$ ; male  $4.60 \pm 0.054$ ) observed at this site. Very low ED responses were observed on account of this low pH. It is important to note that, despite the different response behaviours across different sites, the correlation of sensor ED response with skin surface pH, (as seen in Figs. 3 & 4 for the palm), is expected to be valid at each site, but sensitivity of response is highly site-dependent.

Finally, the gender effect observed in Fig. 3 is also apparent in Fig. 5.

Skin surface pH measurements were consistently lower for males at the palm, foot and abdomen. Despite this lower pH, male sensor spot responses were greater than from females, consistent with what has already been observed. The gender effect was not observed at the forehead as both genders exhibited similar skin surface pH measurements for this site as outlined above.

In order to investigate sensor spot response over time for periods of continuous wear, the wearable platform was worn continuously on the palm for different fixed periods of time up to 270 min (in contrast to the 15 min intervals used in the previous study) and the sensor spots scanned in the usual manner (Fig. 6). This data confirms that the occlusion of the skin is not affecting the pH measurement or the sensor spot response and that the ammonia and volatile amine flux remains constant throughout the sampling period resulting in a cumulative response, which is approximately linear.

To investigate the time dependence on the sensor spot ED response further, a higher number of sensors were worn by a single participant over multiple days (a maximum of one sensor measurement taken per day) for different wear times to better understand both the sensitivity and correlation of sensor response with respect to skin surface pH values measured (Table 1). Sensor ED data ( $n = 7$ ) for each sampling time was plotted against pH and 1-D linear regression applied (SI Fig. 5) to quantify the slope and R. The results show that the ED response increased with wear time as expected and also that both sensitivity and correlation are low for short sampling times (< 60 min) but this

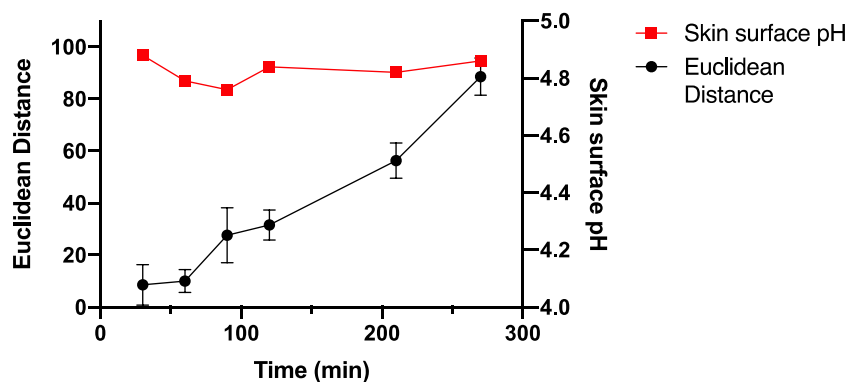


Fig. 6. Average ED colour response from wearable platform (6 replicate BCG sensor spots) worn for different periods of time by a single participant, (female; left palm; average skin surface pH =  $4.82 \pm 0.05$ ). Error bars represent standard deviation in ED response from  $n = 6$  sensor spots within a single wearable platform.

Table 1

1-D linear regression parameters for regression lines fitted to ED colour response as a function of skin surface pH for wearable platforms (6 replicate BCG sensor spots) worn by a single participant collected for continuous sampling times between 30 and 270 min.

Time (min)	Skin surface pH range	No. of measurements	Average ED response	Slope (ED/pH unit)	y-intercept	R
30	4.78–5.09	7	8.72	20.63	−92.88	0.526
60	4.61–5.18	7	17.90	20.82	−85.00	0.689
90	4.67–4.85	7	29.57	84.14	−371.20	0.609
120	4.84–5.13	7	46.07	86.32	−381.70	0.814
210	4.67–5.31	7	83.01	93.75	−369.00	0.767
270	4.78–5.29	7	95.58	93.53	−375.00	0.849

Note: see SI Fig. 5 for ED data and 1-D linear regression analysis of data.

increases with time. For example, the slope was observed to increase 4-fold from 90 min on compared to at 30 min. Correlation was also observed to improve with extended sampling times. These results show that the minimum wear time for these sensors in their current form is 90–120 min to obtain reliable pH data. Work is ongoing to reduce this wear time and/or enhance wearability of the sensor before this simple approach to wearable biondiagnostics can become viable.

In order to investigate how the sensor spots respond to externally applied skin treatments that can temporarily modulate skin pH, various treatments to the skin were investigated for their impact on both skin pH and sensor spot response. Soap, salicylic acid and IPA were all applied as topical treatments and tape-stripping (TS) of the skin to perturb the skin barrier was also carried out according to Methods. Skin surface pH was taken before and after all treatments. Fig. 7 shows the colour changes of the sensor spots after each treatment and the ED response plotted as a function of skin surface pH following treatment. Following all treatments, it can be seen that the sensor underwent a colour change that correlated with change in skin surface pH. For example, the application of salicylic acid resulted in the lowest skin surface pH measurement which correlated with a low ED sensor response. In contrast, soap elevated the skin surface pH, again correlating with a high ED response. There is high variability noted in the ED response for the soap data in particular despite the study being carried out on a single participant. This may be due to the procedure for washing of the skin with soap where, e.g., the ratio of water:soap used for each treatment was not controlled and may have contributed variability to the sensor response. IPA application and tape-stripping both lowered the skin surface pH by small amounts relative to the control, resulting in a correlated small reduction in ED response. These experiments demonstrate that skin surface pH and the corresponding volatile profile is altered temporarily by these treatments and that these alterations can be tracked using our wearable colorimetric sensor spot platform.

#### 4. Conclusion

The application of a simple wearable platform incorporating pH-

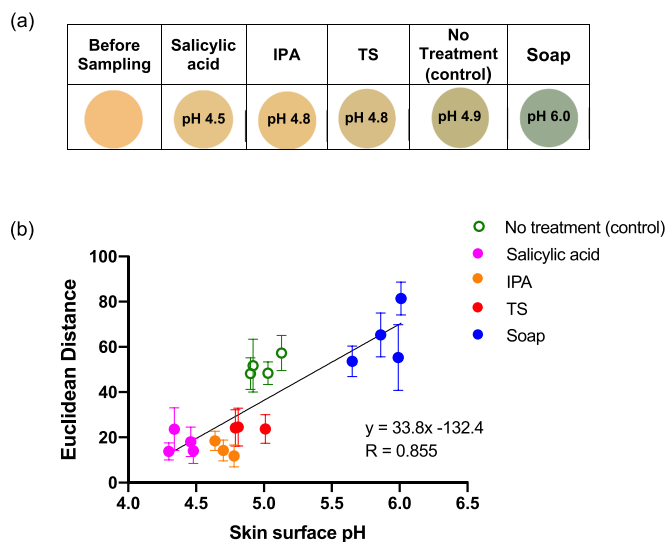


Fig. 7. (a) Reproduced colour (average of 6 replicate BCG sensor spots) following 120 min sampling time on palm of a single female participant for untreated skin and following various treatments, and (b) average ED colour response from wearable platform as a function of skin surface pH. Error bars represent standard deviation in ED response from  $n = 6$  sensor spots within a single wearable platform.

responsive sensor spots for the measurement of skin surface pH via the volatile ammonia emission from skin in a healthy participant study was reported. Overall, this work explores the potential use of the volatile emission from skin, the exciting opportunities as well as the challenges for such a sensing approach in wearable biondiagnostics. Our wearable sensor was investigated for healthy participant skin surface pH measurements, and gender and body site differences were attributed to gland type and distribution densities as well as potential microbial influences. Our findings demonstrate that such wearable colorimetric

sensor platforms can be used to selectively monitor target components of the skin volatile emission and offers an alternative to skin fluid harvesting and analysis. This work also highlights challenges associated with the approach such as inter-person variability in the sensor ED response. Also, the impacts of skin occlusion by wearables need to be considered as it can trigger a sweat response from the skin, potentially interfering with the sensor response. Ideally, sensors for these measurements require short response times or have a form factor that does not occlude the skin. Furthermore, an in-situ or even wearable imaging approach will further enhance these colour sensors deployability and potential use which is currently being developed in our group.

Despite these challenges, the development of this new wearable paves the way for demonstrating the concept of harnessing diagnostic information from the skin volatile emission as well as motivating the use of alternate colour chemistries for targeting other volatile biomarkers such as aldehydes for the monitoring of states including ketosis and oxidative stress for example. The development of such simple, colour-based wearable sensing approaches could prove useful in personalised monitoring of general health and also for self-management of chronic diseases associated with volatile biomarkers in the future.

### Declaration of Competing Interest

The authors declare that they have no known competing financial interests or personal relationships that could have appeared to influence the work reported in this paper.

### Acknowledgements

M Finnegan would like to acknowledge funding support from the Insight SFI Research Centre for Data Analytics under Science Foundation Ireland (SFI); Grant Number SFI/12/RC/2289\_P2, co-funded by the European Regional Development Fund. E Duffy was supported by funding from the European Union's Horizon 2020 Research and Innovation programme under the Marie Skłodowska-Curie Grant Agreement Number 796289.

### Appendix A. Supplementary data

Supplementary data to this article can be found online at <https://doi.org/10.1016/j.sbsr.2022.100473>.

### References

- [1] C. Drislane, A.D. Irvine, The role of flaggrin in atopic dermatitis and allergic disease, *Ann. Allergy Asthma Immunol.* 124 (2020) 36–43.
- [2] B. Piro, G. Mattana, V. Noël, Recent advances in skin chemical sensors, *Sensors* 19 (2019) 4376.
- [3] E. Duffy, A. Morrin, Endogenous and microbial volatile organic compounds in cutaneous health and disease, *TrAC Trends Anal. Chem.* 111 (2019) 163–172.
- [4] J. Heikenfeld, A. Jajack, B. Feldman, S.W. Granger, S. Gaitonde, G. Begtrup, B. A. Katchman, Accessing analytes in biofluids for peripheral biochemical monitoring, *Nat. Biotechnol.* 37 (2019) 407–419.
- [5] J.I. Joseph, Review of the long-term implantable senseonics continuous glucose monitoring system and other continuous glucose monitoring systems, *J. Diabetes Sci. Technol.* 15 (2021) 167–173.
- [6] R. Ghaffari, J.A. Rogers, T.R. Ray, Recent progress, challenges, and opportunities for wearable biochemical sensors for sweat analysis, *Sensors Actuators B Chem.* 332 (2021) 129447.
- [7] J. Heikenfeld, A. Jajack, J. Rogers, P. Gutruf, L. Tian, T. Pan, R. Li, M. Khine, J. Kim, J. Wang, J. Kim, Wearable sensors: modalities, challenges, and prospects, *Lab Chip* 18 (2018) 217–248.
- [8] P. Escobedo, C.E. Ramos-Lorente, A. Martínez-Olmos, M.A. Carvajal, M. Ortega-Muñoz, I. de Orbe-Payá, F. Hernández-Mateo, F. Santoyo-González, L.F. Capitán-Vallvey, A.J. Palma, M.M. Erenas, Wireless wearable wristband for continuous sweat pH monitoring, *Sensors Actuators B Chem.* 327 (2021), 128948.
- [9] J. Kim, A.S. Campbell, J. Wang, Wearable non-invasive epidermal glucose sensors: a review, *Talanta* 177 (2018) 163–170.
- [10] A.J. Bandodkar, W. Jia, C. Yardımcı, X. Wang, J. Ramirez, J. Wang, Tattoo-based noninvasive glucose monitoring: a proof-of-concept study, *Anal. Chem.* 87 (2015) 394–398.

- [11] W. Jia, A.J. Bandodkar, G. Valdés-Ramírez, J.R. Windmiller, Z. Yang, J. Ramirez, G. Chan, J. Wang, Electrochemical tattoo biosensors for real-time noninvasive lactate monitoring in human perspiration, *Anal. Chem.* 85 (2013) 6553–6560.
- [12] I. Shitanda, M. Mitsumoto, N. Loew, Y. Yoshihara, H. Watanabe, T. Mikawa, S. Tsujimura, M. Itagaki, M. Motosuke, Continuous sweat lactate monitoring system with integrated screen-printed MgO-templated carbon-lactate oxidase biosensor and microfluidic sweat collector, *Electrochim. Acta* 368 (2021), 137620.
- [13] J.R. Sempionatto, T. Nakagawa, A. Pavinatto, S.T. Mensah, S. Imani, P. Mercier, J. Wang, Eyeglasses based wireless electrolyte and metabolite sensor platform, *Lab Chip* 17 (2017) 1834–1842.
- [14] S. Bong Kim, J. Koo, J. Yoon, A. Hourlier-Fargette, B. Lee, S. Chen, S. Jo, J. Choi, Oh.Y. Suk, G. Lee, S. Min Won, J.A. Aranyosi, S.P. Lee, J.B. Model, P.V. Braun, R. Ghaffari, C. Park, J.A. Rogers, Soft, skin-interfaced microfluidic systems with integrated enzymatic assays for measuring the concentration of ammonia and ethanol in sweat, *Lab Chip* 20 (2020) 84–92.
- [15] Z. Sonner, E. Wilder, J. Heikenfeld, G. Kasting, F. Beyette, D. Swaile, F. Sherman, J. Joyce, J. Hagen, N. Kelley-Loughnane, R. Naik, The microfluidics of the eccrine sweat gland, including biomarker partitioning, transport, and biosensing implications, *Biomicrofluidics* 9 (2015), 031301.
- [16] S.R. Corrie, J.W. Coffey, J. Islam, K.A. Markey, M. Kendall, Blood, sweat, and tears: developing clinically relevant protein biosensors for integrated body fluid analysis, *Analyst* 140 (2015) 4350–4364.
- [17] N. Kashaninejad, A. Munaz, H. Moghadas, S. Yadav, M. Umer, N.-T. Nguyen, Microneedle arrays for sampling and sensing skin interstitial fluid, *Chemosensors* 9 (2021) 83.
- [18] K.Y. Goud, C. Moonla, R.K. Mishra, C. Yu, R. Narayan, I. Litvan, J. Wang, Wearable electrochemical microneedle sensor for continuous monitoring of Levodopa: toward Parkinson management, *ACS Sens.* 4 (2019) 2196–2204.
- [19] T. Glennon, C. O'Quigley, M. McCaul, G. Matzeu, S. Beirne, G.G. Wallace, F. Stroiescu, N. O'Mahoney, P. White, D. Diamond, 'SWEATCH': A wearable platform for harvesting and analysing sweat sodium content, *Electroanalysis* 28 (2016) 1283–1289.
- [20] P. Pirovano, M. Dorrian, A. Shinde, A. Donohoe, A.J. Brady, N.M. Moyna, G. Wallace, D. Diamond, M. McCaul, A wearable sensor for the detection of sodium and potassium in human sweat during exercise, *Talanta* 219 (2020), 121145.
- [21] A.J. Bandodkar, P. Gutruf, J. Choi, K. Lee, Y. Sekine, J.T. Reeder, W.J. Jeang, A. J. Aranyosi, S.P. Lee, J.B. Model, R. Ghaffari, C.-J. Su, J.P. Leshock, T. Ray, A. Verrillo, K. Thomas, V. Krishnamurthi, S. Han, J. Kim, S. Krishnan, T. Hang, J. A. Rogers, Battery-free, skin-interfaced microfluidic/electronic systems for simultaneous electrochemical, colorimetric, and volumetric analysis of sweat, *Sci. Adv.* 5 (2019) (eaav3294).
- [22] A. Martín, J. Kim, J.F. Kurniawan, J.R. Sempionatto, J.R. Moreto, G. Tang, A. S. Campbell, A. Shin, M.Y. Lee, X. Liu, J. Wang, Epidermal microfluidic electrochemical detection system: enhanced sweat sampling and metabolite detection, *ACS Sens.* 2 (2017) 1860–1868.
- [23] L. Dormont, J.-M. Bessi re, A. Cohuet, Human skin volatiles: a review, *J. Chem. Ecol.* 39 (2013) 569–578.
- [24] N. Drabińska, C. Flynn, N. Ratcliffe, I. Belluomo, A. Myridakis, O. Gould, M. Fois, A. Smart, T. Devine, B.D.L. Costello, A literature survey of all volatiles from healthy human breath and bodily fluids: the human volatilome, *J. Breath Res.* 15 (2021), 034001.
- [25] D.J. Penn, E. Oberzaucher, K. Grammer, G. Fischer, H.A. Soini, D. Wiesler, M. V. Novotny, S.J. Dixon, Y. Xu, R.G. Brereton, Individual and gender fingerprints in human body odour, *J. R. Soc. Interface* 4 (2007) 331–340.
- [26] B. Grabowska-Polanowska, P. Miarka, M. Skowron, J. Sułowicz, K. Wojtyna, K. Moskal, I. Śliwka, Development of sampling method and chromatographic analysis of volatile organic compounds emitted from human skin, *Bioanalysis* 9 (2017) 1465–1475.
- [27] A.P. Roodt, Y. Naud , A. Stoltz, E. Rohwer, Human skin volatiles: passive sampling and GC × GC-ToFMS analysis as a tool to investigate the skin microbiome and interactions with anthropophilic mosquito disease vectors, *J. Chromatogr. B* 1097–1098 (2018) 83–93.
- [28] Z.-M. Zhang, J.-J. Cai, G.-H. Ruan, G.-K. Li, The study of fingerprint characteristics of the emanations from human arm skin using the original sampling system by SPME-GC/MS, *J. Chromatogr. B* 822 (2005) 244–252.
- [29] E. Duffy, M.R. Jacobs, B. Kirby, A. Morrin, Probing skin physiology through the volatile footprint: discriminating volatile emissions before and after acute barrier disruption, *Exp. Dermatol.* 26 (2017) 919–925.
- [30] E. Duffy, K.D. Guzman, R. Wallace, R. Murphy, A. Morrin, Non-invasive assessment of skin barrier properties: investigating emerging tools for in vitro and in vivo applications, *Cosmetics* 4 (2017) 44.
- [31] T. Shetewi, M. Finnegan, S. Fitzgerald, S. Xu, E. Duffy, A. Morrin, Investigation of the relationship between skin-emitted volatile fatty acids and skin surface acidity in healthy participants – a pilot study, *J. Breath Res.* 15 (2021) 037101.
- [32] S.G. Danby, M.J. Cork, pH in Atopic Dermatitis *pH of the Skin: Issues and Challenges* 54, 2018, pp. 95–107.
- [33] T. Knor, A. Meholfjić-Fetahović, A. Mehmedagić, Stratum corneum hydration and skin surface pH in patients with atopic dermatitis, *Acta Dermatovenerol. Croat.* 19 (2011) 242–247.
- [34] E. Proksch, pH in nature, humans and skin, *J. Dermatol.* 45 (2018) 1044–1052.
- [35] K. Nose, T. Mizuno, N. Yamane, T. Kondo, H. Ohtani, S. Araki, T. Tsuda, Identification of ammonia in gas emanated from human skin and its correlation with that in blood, *Anal. Sci.* 21 (2005) 1471–1474.
- [36] M.G. Bulmer, The concentration of urea in thermal sweat, *J. Physiol.* 137 (1957) 261–266.

- [37] A. Watabe, T. Sugawara, K. Kikuchi, K. Yamasaki, S. Sakai, S. Aiba, Sweat constitutes several natural moisturizing factors, lactate, urea, sodium, and potassium, *J. Dermatol. Sci.* 72 (2013) 177–182.
- [38] P. Martínez-Lozano, Mass spectrometric study of cutaneous volatiles by secondary electrospray ionization, *Int. J. Mass Spectrom.* 282 (2009) 128–132.
- [39] U.R. Bernier, D.L. Kline, D.R. Barnard, C.E. Schreck, R.A. Yost, Analysis of human skin emanations by gas chromatography/mass spectrometry. 2. Identification of volatile compounds that are candidate attractants for the yellow fever mosquito (*Aedes aegypti*), *Anal. Chem.* 72 (2000) 747–756.
- [40] S. Furukawa, Y. Sekine, K. Kimura, K. Umezawa, S. Asai, H. Miyachi, Simultaneous and multi-point measurement of ammonia emanating from human skin surface for the estimation of whole body dermal emission rate, *J. Chromatogr. B* 1053 (2017) 60–64.
- [41] M. Li, C.J. Weschler, G. Bekö, P. Wargocki, G. Lucic, J. Williams, Human ammonia emission rates under various indoor environmental conditions, *Environ. Sci. Technol.* (2020) 10.
- [42] J. Xiao, Y. Liu, L. Su, D. Zhao, L. Zhao, X. Zhang, Microfluidic chip-based wearable colorimetric sensor for simple and facile detection of sweat glucose, *Anal. Chem.* 91 (2019) 14803–14807.
- [43] J. Choi, D. Kang, S. Han, S.B. Kim, J.A. Rogers, Thin, soft, skin-mounted microfluidic networks with capillary bursting valves for Chrono-sampling of sweat, *Adv. Healthc. Mater.* 6 (2017) 1601355.
- [44] A. Koh, D. Kang, Y. Xue, S. Lee, R. Pielak, J. Kim, T. Hwang, S. Min, A. Banks, P. Bastien, M. Manco, L. Wang, K. Ammann, K.-I. Jang, P. Won, S. Han, R. Ghaffari, U. Paik, M. Slepian, J. Rogers, A soft, wearable microfluidic device for the capture, storage, and colorimetric sensing of sweat, *Sci. Transl. Med.* 8 (2016) (366ra165–366ra165).
- [45] Y. Zhang, H. Guo, S.B. Kim, Y. Wu, D. Ostojich, S.H. Park, X. Wang, Z. Weng, R. Li, A.J. Bandodkar, Y. Sekine, J. Choi, S. Xu, S. Quaggin, R. Ghaffari, J.A. Rogers, Passive sweat collection and colorimetric analysis of biomarkers relevant to kidney disorders using a soft microfluidic system, *Lab Chip* 19 (2019) 1545–1555.
- [46] K.S. Suslick, N.A. Rakow, A. Sen, Colorimetric sensor arrays for molecular recognition, *Tetrahedron* 60 (2004) 11133–11138.
- [47] D.F. Hamilton, M. Gherl, A.H.R.W. Simpson, Interpreting regression models in clinical outcome studies, *Bone Joint Res.* 4 (2015) 152–153.
- [48] P.A. Low, in: D. Robertson, I. Biaggioni, G. Burnstock, P.A. Low, J.F.R. Paton (Eds.), Chapter 51 - Sweating *Primer on the Autonomic Nervous System*, Third ed., Academic Press, San Diego, 2012, pp. 249–251.
- [49] N.A. Taylor, C.A. Machado-Moreira, Regional variations in transepidermal water loss, eccrine sweat gland density, sweat secretion rates and electrolyte composition in resting and exercising humans, *Extrem. Physiol. Med.* 2 (2013) 4.
- [50] M. Harker, Psychological sweating: a systematic review focused on aetiology and cutaneous response, *Skin Pharmacol. Physiol.* 26 (2013) 92–100.
- [51] A. SanMiguel, E.A. Grice, Interactions between host factors and the skin microbiome, *Cell. Mol. Life Sci.* 72 (2015) 1499–1515.
- [52] G. Shamloul, A. Khachemoune, An updated review of the sebaceous gland and its role in health and diseases part 1: embryology, evolution, structure, and function of sebaceous glands, *Dermatol. Ther.* 34 (2021) (e14695).